AMERICAN SOCIETY FOR MICROBIOLOGY | Applied and Environmental Microbiology

Microbial Mat Communities along an Oxygen Gradient in a Perennially Ice-Covered Antarctic Lake

Anne D. Jungblut,[a] Ian Hawes,[b] Tyler J. Mackey,[c] Megan Krusor,[d] Peter T. Doran,[e] Dawn Y. Sumner,[c] Jonathan A. Eisen,[d,e] Colin Hillman,[b] Alexander K. Goroncy[b]

Life Sciences Department, The Natural History Museum, London, United Kingdom[a]; University of Canterbury, Christchurch, New Zealand[b]; Department of Earth and Planetary Sciences, University of California, Davis, Davis, California, USA[c]; Microbiology Graduate Group, University of California, Davis, Davis, California, USA[d]; Department of Geology and Geophysics, Louisiana State University, Baton Rouge, Louisiana, USA[e]

Lake Fryxell is a perennially ice-covered lake in the McMurdo Dry Valleys, Antarctica, with a sharp oxycline in a water column that is density stabilized by a gradient in salt concentration. Dissolved oxygen falls from 20 mg liter^{-1} to undetectable over one vertical meter from 8.9- to 9.9-m depth. We provide the first description of the benthic mat community that falls within this oxygen gradient on the sloping floor of the lake, using a combination of micro- and macroscopic morphological descriptions, pigment analysis, and 16S rRNA gene bacterial community analysis. Our work focused on three macroscopic mat morphologies that were associated with different parts of the oxygen gradient: (i) "cuspate pinnacles" in the upper hyperoxic zone, which displayed complex topography and were dominated by phycoerythrin-rich cyanobacteria attributable to the genus *Leptolyngbya* and a diverse but sparse assemblage of pennate diatoms; (ii) a less topographically complex "ridge-pit" mat located immediately above the oxic-anoxic transition containing *Leptolyngbya* and an increasing abundance of diatoms; and (iii) flat prostrate mats in the upper anoxic zone, dominated by a green cyanobacterium phylogenetically identified as *Phormidium pseudopriestleyi* and a single diatom, *Diadesmis contenta*. Zonation of bacteria was by lake depth and by depth into individual mats. Deeper mats had higher abundances of bacteriochlorophylls and anoxygenic phototrophs, including *Chlorobi* and *Chloroflexi*. This suggests that microbial communities form assemblages specific to niche-like locations. Mat morphologies, underpinned by cyanobacterial and diatom composition, are the result of local habitat conditions likely defined by irradiance and oxygen and sulfide concentrations.

The McMurdo Dry Valleys (MDV) region of Southern Victoria Land, Antarctica, contains a number of perennially ice-covered lakes, each home to complex and diverse microbial communities (1). Unusual properties of these lakes, which are sustained by the year-round ice cover, include the absence of wind-induced turbulence and persistent, salinity-dependent density gradients, which often encompass a significant proportion of the lake water columns (2). These properties make the MDV lake systems among the most physically stable lacustrine habitats on Earth, and research over the past decades has shown that microbial communities and processes are consistently embedded at specific positions in environmental gradients within their stable water columns (e.g., 3). There is a strong connection between dominant microbial physiologies and redox-related biogeochemistry through the water column (4–9), and microbial distributions along stable redox gradients have provided useful test cases for understanding links between environment and metabolism. To date, such observations have largely been confined to planktonic communities (3, 6, 10), despite the fact that in all MDV lakes studied, thick microbial mats cover the floors of the lakes to the base of the photic zone. In Lakes Hoare and Vanda, these benthic mats have been estimated to contribute at least as much biomass and biological productivity, on a whole-lake basis, as plankton (11–15).

Previous work on microbial mat community composition in MDV lakes has focused almost exclusively on the oxygenic communities, dominated by cyanobacteria, in the upper parts of the lakes. Two distinct mats zones are recognized. Below the ice cover, where liquid water persists year round, mats are rich in light-harvesting pigments (12) and extracellular polysaccharides, are laminated (11), and often take the form of complex, three-dimensional structures (13, 16, 17). During summer, solar heating melts the shallow margins of most MDV lakes to some extent, creating shallow "moats" that seasonally alternate between ice free and frozen. Here, mat morphological complexity is suppressed and communities are acclimated to much higher irradiance (e.g., 11, 18). Approaches to community assemblage analysis in both zones have been based primarily on microscopy and have shown that mats provide habitats for cyanobacteria, microbial eukaryotes, microalgae, and heterotrophic bacteria (19, 20). Though molecular methods applied to cyanobacterial diversity have confirmed an assemblage dominated by *Oscillatoriales* and *Nostocales* in mats from moats (21), mats growing on the sloping lake floors from the underside of the ice to greater depths were dominated by *Oscillatoriales*, with most variation in diversity being related to irradiance and conductivity (22).

To date, while some effort has been made to understand

Received 21 August 2015 **Accepted** 2 November 2015

Accepted manuscript posted online 13 November 2015

Citation Jungblut AD, Hawes I, Mackey TJ, Krusor M, Doran PT, Sumner DY, Eisen JA, Hillman C, Goroncy AK. 2016. Microbial mat communities along an oxygen gradient in a perennially ice-covered Antarctic lake. Appl Environ Microbiol 82:620–630. doi:10.1128/AEM.02699-15.

Editor: A. J. Stams

Address correspondence to Anne D. Jungblut, a.jungblut@nhm.ac.uk.

Supplemental material for this article may be found at http://dx.doi.org/10.1128/AEM.02699-15.

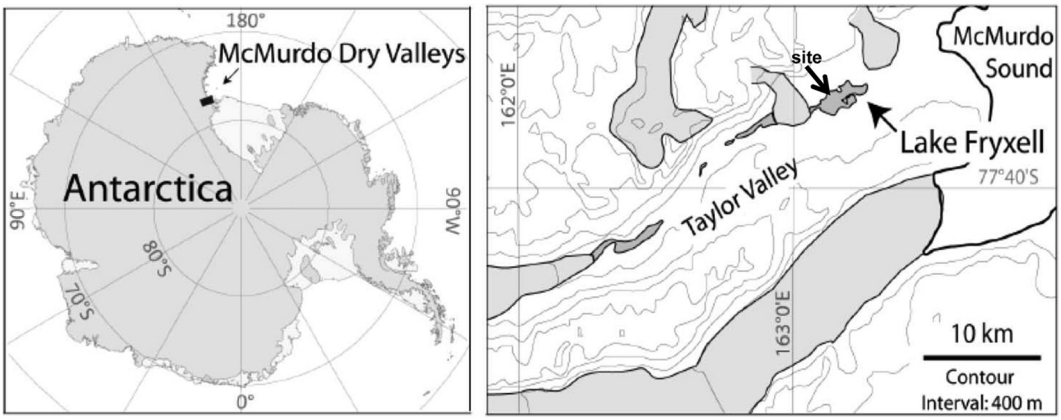

FIG 1 Locations of the McMurdo Dry Valley region of continental Antarctica and of Lake Fryxell and the dive site in Taylor Valley. (Adapted from reference 28.)

changes within the cyanobacterial community at different lake depths in the MDV lakes, this has not extended into the anoxic or micro-oxic parts of the water column (12, 23, 24). In traversing the oxycline, we expect a change in microbial community, both functionally and compositionally, as described for planktonic communities (25). Furthermore, it is not known how the composition and dominant metabolisms of bacteria other than cyanobacteria shift with lake depth or redox gradients and how these changes might relate to observed shifts in macroscopic mat morphology with lake depth (18). The goal of this study was to address this gap by describing the benthic community across the oxycline in Lake Fryxell, an MDV lake.

Lake Fryxell is among the better-studied MDV lakes, particularly from the perspective of anoxic microbiology (7). It has a stable geochemical and salinity stratification (26), within which dissolved oxygen falls from 20 mg liter^{-1} close to the ice cover to undetectable at a readily accessible 9- to 10-m depth (27). This transition coincides with increasing sulfide and a shift from oxygen- to sulfur-based water column metabolism (7). Lake Fryxell also has a gently sloping lake floor colonized by microbial mats, and therefore vertically steep geochemical gradients translate to relatively long and readily sampled horizontal distances.

In the present study, our aim was therefore to describe the mat composition, including cyanobacteria, other bacteria, and archaea, and the macroscopic mat morphology along a transect from oxic to anoxic conditions in Lake Fryxell using a combination of morphological descriptions, pigment analysis, and next-generation sequencing of 16S rRNA genes for community analysis. As part of the description of the mat communities in Lake Fryxell, we identified a highly abundant cyanobacterium that occupies a unique niche below the oxycline where it produces an oxygenated "oasis" (28), and we therefore undertook a comprehensive phylogenetic analysis of this organism.

MATERIALS AND METHODS

Study site. Lake Fryxell (77°36′S, 162°6′E) (Fig. 1) is located near the eastern end of Taylor Valley. It is a meromictic lake where water layers do not intermix. It is 5 by 1.5 km in extent and permanently covered by 4.5 m of ice (7, 27). The maximum depth is ~20 m, including the ice cover. Water is supplied to Lake Fryxell by 13 glacial meltwater streams, with most water coming from the Canada and Commonwealth glaciers (29). Water balance is achieved by evaporation and ablation from the surface, and there are no outflowing streams (30).

Like for most lakes of the MDV, the level of Lake Fryxell has fluctuated over time, which is reflected in its current physical structure. It has been suggested that 24,000 years ago, Lake Fryxell formed part of a large water body (Lake Washburn). Prior to ca. 1,000 years ago, Lake Fryxell may have evaporated to a small playa before inflowing meltwater flooded over this brine (31). Though recent research has questioned the full extent of this dry-down (32), it seems certain that the lake has had a series of relatively low-level events, with evaporation to at least 5 m below present lake level (33). The legacy of these evaporation-refilling events is a salinity gradient from the floor of the lake to the underside of the ice and an inherently stable water column (2). Physical mixing is weak at best in large sections of lake water column (10), and vertical flux of solutes occurs largely by diffusion rather than turbulence (34).

The ice cover of Lake Fryxell has been shown to transmit a few percent of incident irradiance (35), which is sufficient to support a deep chlorophyll (Chl) maximum reaching >20 mg m^{-3} (27) just above the oxygen limit/nutricline, which is at 9- to 11-m depth (10, 36). Based on studies to date, benthic phototrophic microbial mats appear to be present to depths of at least 10.5 m all around the lake (18).

Sample collection. Sampling was undertaken in November 2012 by divers operating through a single hole melted in the ice cover on the northern side of the lake, at 77°36.4′S, 163°09.1′E (Fig. 1). In November 2006, a transect was established and marked by a rope from 8.9- to 11.0-m depth (all depths are based on the hydrostatic water level in November 2012). Nine stations along the transect were marked with pegs between 8.9- and 11-m depth (Table 1). The dive hole in 2012 was over 8 m of water near the transect, and all sampling was undertaken at transect stations unless stated otherwise. The gentle slope of the lake bottom at the transect site meant that the vertical drop of 3 m corresponded to a horizontal distance of ~50 m.

Physical properties. Irradiance at each transect station was determined by a diver equipped with surface communications carrying a Li-Cor Li 1400 m in a waterproof housing, to which a Li 192 photosynthetically active radiation (PAR) sensor was connected. As underwater measurements were made, simultaneous measurement of irradiance incident to the lake surface (Li 190 PAR sensor) allowed the percent surface irradiance to be calculated. The attenuation coefficient for downwelling radiation was determined from these observations and transect station depth (see below) by log-linear regression analysis (37). The transmission of the ice cover was measured similarly but with the underwater sensor held up to the underside of the ice cover while the diver swam a series of radial patterns from the dive hole, taking care to avoid the area of unnaturally bright ice close to the dive hole.

TABLE 1 Physical and chemical variables along the depth transect in Lake Fryxell[a]

Station	Depth (m)	EC (mS cm^{-1})	DO (mg liter^{-1})	Irradiance (% surface)	pH	DIC (mg liter^{-1})	DRP (μg liter^{-1})	NH_4 N (μg liter^{-1})	$NO_2 + NO_3^-$ N (μg liter^{-1})
1	8.9	2.98	20.4	0.74	7.50	15.5	2	<1[b]	1
2	9.0	3.04	15.2	0.82	7.47	14.4	2	<1	1
3	9.3	3.15	7.4	0.44	7.46	16.1	1	<1	1
4	9.4	3.33	4.5	0.36	7.44	18.0	2	<1	1
5	9.7	3.54	0.2	0.26	7.48	20.2	3	8	1
6	9.9	3.61	0	0.27	7.49	20.9	3	13	1
7	10.2	3.90	0	0.22	7.47	21.6	39	100	1
8	10.6	4.25	0	0.18	7.51	23.2	53	120	1
9	11.0	4.61	0	0.12	7.52	26.0	70	280	2

[a] EC, electrical conductivity; DO, dissolved oxygen; DIC, dissolved inorganic carbon; DRP, dissolved reactive phosphorus.
[b] <1, below limit of detection.

Conductivity-temperature-depth-oxygen (CTDO) profiles were obtained in November 2012 using a recently calibrated Richard Brancker "Concerto" CTD, recording at 6 Hz, to which was attached a Unisense UWM picoammeter recording signals at 1 Hz from a Unisense oxygen microelectrode (38). The microelectrode had a 50-μm-diameter tip and a 90% response time of <2 s. It was calibrated at ambient temperature against air-saturated distilled water and water deoxygenated using sodium dithionite. The combined instrument was first lowered though a hole in the lake ice close to the deepest part of the lake to obtain a continuous CTDO cast. Postprocessing aligned data from the two instruments by time, using a 6-point running mean for the CTD data to accommodate the higher sampling rate. To determine the conditions along the benthic transect, the combined instrument was later carried along the transect by a diver and lowered to within 50 mm of the lake floor at each station while recording continuously, as described above, with the time stamp of each instrument record used to reconcile location and data. These data were used to confirm the depths of the transect sites.

Water chemistry. Water samples were taken at each station using acid-washed 60-ml syringes. Divers drew water into the syringes while the syringes were held just above the lake bottom, rinsing them thrice prior to collecting water samples. Once returned to the lake surface, one syringe sample from each depth was analyzed immediately for pH using a calibrated portable meter. Three replicate samples of 2 ml of lake water from this syringe were also injected into 12-ml serum tubes, preloaded with 0.2 ml concentrated phosphoric acid, for subsequent determination of dissolved inorganic carbon (DIC). Prior to sample injection, a suitable volume of air was withdrawn from the tubes to ensure approximate pressure equilibrium after sample injection. A second syringe of water was filtered (Whatman GF/F) directly into an acid-washed high-density polyethylene (HDPE) bottle and frozen in a portable freezer at −20°C. Bottles were transported frozen to New Zealand and stored at −20°C until nutrients were analyzed.

Upon return to New Zealand, DIC was measured as CO_2 by injecting a subsample of the headspace directly into a stream of nitrogen gas, which then passed through the measuring channel of a Li-Cor infrared gas analyzer (IRGA). The DIC concentration was estimated from peak height using suitable blanks and bicarbonate calibration standards. Frozen water samples were melted, and NH_4^+ N, NO_2^- plus NO_3^- N, and dissolved reactive phosphorus (DRP) were measured using an Astoria autoanalyzer.

Classification and quantification of macroscopic mat morphology. The macroscopic characteristics of the microbial mats on the bottom of Lake Fryxell were recorded by a diver who operated a downward-facing high-resolution digital video camera (Go-Pro HD Hero 2), a light-emitting diode (LED) light source, the Brancker CTD for depth recording, and two parallel lasers spaced 3 cm apart for scale. The CTD measured the depth of the camera at 1-s intervals, which allowed subsequent depth referencing of time-stamped video frames. Laser pointers were offset at an angle to the video camera to allow calculation of camera height above the mat surface from the location of the laser points in the camera field of view. Distance from the lake floor was calibrated using images obtained at 11 defined distances from a gridded calibration target. The absolute depth of the lake floor at a given point was calculated based on the CTD depth and distance above the lake floor, which was calculated from the laser positions in the image. Calculated depths were cross-checked at three staked sites along the transect, and the error was <100 mm.

The mat morphology survey involved a diver swimming a series of meandering tracks through a 25-m-wide swath to one side of the transect. Recorded images were reviewed and used to produce a mat typology based on dominant features, including presence or absence of pinnacles or ridges, color, and texture. A total of 197 frames along the video transects were then scored for lake depth and mat type at the point where the laser scale impinged on the mat surface, and mat type frequencies were compiled for 0.1-m-depth bins.

Representative mat samples were collected by divers and vertically sectioned to document lamination of the main mat morphologies present along the transect. The dominant cyanobacterial morphotypes in different microbial mat sections were identified on site using an Olympus light microscope (BX51; Olympus) at magnifications of ×400 to ×1,000 and were assigned to genera as described by Komarek and Anagnostidis (39–41).

Pigment and diatom analysis. Samples for quantitative pigment and diatom analysis were taken with a 38-mm-diameter corer, with four replicates at each transect station. Individual cores were placed into a 60-ml wide-mouthed bottle underwater, sealed, and returned to the surface. On-site processing involved draining excess water and freezing (−20°C). Upon return to New Zealand, samples were freeze-dried and ground to a fine powder. Weighed aliquots were used for phycoerythrin and chlorophyll analyses, pigment high-pressure liquid chromatography (HPLC), and diatom relative abundance counts.

For the phycoerythrin analysis, aliquots were extracted into 5 ml 0.1 M Tris buffer (pH 7.6) using ultrasonication (15 W for 30 s) in an ice-water bath and left to extract at 4°C for 12 to 16 h. After clarification by filtration (Whatman GF/F), extracts were analyzed fluorometrically as described by Downes and Hall (42). Subsamples for chlorophyll were extracted by sonication in ice-cold 95% acetone and left at 4°C in the dark for 12 to 16 h to complete extraction. After clarification by centrifugation, the chlorophyll concentration was initially determined by spectrophotometry at 665 nm, without acidification using a method designed for chlorophyll *a* (Chl *a*) (43). This method uses absorption of extracts at 750 nm as a reference wavelength to correct extracts for other absorbing material, since Chl *a* does not absorb at 750 nm. However, the main portion of extracts had distinct absorption peaks close to 750 nm, which we inferred to be due to bacteriochlorophyll *a* (Bchl *a*). Thus, this correction step was excluded. Instead, absorption at 755 nm was recorded, and Bchl *a* was estimated using the absorption coefficient given by Scheer (44). HPLC analysis was carried out as described by Hawes et al. (45), and Bchl *c*, Bchl *d*, and Bchl

e were identified using diode array spectra (400 to 800 nm) and extinction maxima assembled by Scheer (44). The absorption of each of these pigments at 665 nm was recorded, and the percent contributions of Chl *a*, Bchl *c*, Bchl *d*, and Bchl *e* to the measured 665-nm absorption were calculated, assuming absorption to be additive.

To identify diatoms, a third subsample from each the four replicates was cleaned in three overnight rinses of 14% hydrogen peroxide, mounted in Naphrax, and inspected using a Leitz light microscope at magnifications of ×400 to ×1,000. For each sample, the relative abundance of diatoms was calculated based on identification of 200 frustules in transects across prepared slides. Identifications were made by reference to the work of Spaulding et al. (46), and Shannon's diversity index was calculated for each sample.

Mat collection for molecular analysis, DNA extraction, MiSeq sequencing, and 16S rRNA gene community structure analysis. Triplicate microbial mat samples representing the main three macroscopic mat morphologies, i.e., cuspate pinnacle, ridge-pit, and prostrate, were collected by a diver by cutting squares of mat from the lake floor and gently lifting them into a plastic box previously cleaned with antibacterial wipes. Box lids were sealed under water and samples returned to the surface and transferred to lakeside laboratory, where they were immediately dissected using flame-sterilized blades and forceps. Pinnacle and ridge-pit mats were dissected according to their distinctively pigmented horizontal upper (pink-purple and brown-purple, respectively), middle (pale purple and green-beige, respectively), and lower (all beige) layers. Prostrate mats were similarly dissected into upper (brown-purple), middle (green-beige), and lower (beige) layers. Dissected subsamples were rinsed in sterile deionized water, transferred into sterile plastic tubes, and frozen at −20°C until further analysis.

DNA extractions of each of the triplicate mat sections were performed using the MoBio PowerDNA biofilm kit according to the manufacturer's instructions. DNA was quantified using a Qubit fluorometer, and equal amounts of DNA per sample were pooled for 16S rRNA gene amplification. 16S rRNA gene PCR products were amplified (47) in triplicate, pooled, and cleaned using the MoBio UltraClean PCR clean-up kit according to the manufacturer's instructions. For the high-throughput sequencing, we used primers (515f and 806r), described by Caporaso et al. (47), which amplify both archaeal and bacterial 16S rRNA genes, including cyanobacterial 16S rRNA genes. Sequencing was performed on a MiSeq Illumina sequencer at NZ Genomics Limited, Palmerston North, New Zealand. Low-quality reads were removed using the Perl script DynamicTrim (part of the SolexaQA package, v. 2.0) (48), and the quality level was set at a *P* value of 0.001. Paired-end sequences were generated using FLASH (v. 1.2.2) (49), looking for reads of 253 ± 3 bp. QIIME v. 1.8.0 (47) was used to generate operational taxonomic units (OTUs) and perform open-reference OTU picking. Paired-end sequences were aligned using PyNast v. 1.2.2 (50). OTUs with fewer than 10 reads and chimeras were excluded from further analyses. The remaining OTUs were assigned using SILVA (51). Diversity indices, rarefaction curves, and nonmetric multidimensional scaling (NMDS) were calculated using R (vegan package) (52). NMDS was performed using weighted normalized UniFrac distance and 1,000 permutations.

Isolation and phylogenetic analysis of a *Phormidium* cyanobacterium. A blue-green filamentous cyanobacterial film was removed from the upper surface of a prostrate microbial mat (10.4-m depth) for isolation using sterile forceps. It was confirmed by microscopic inspection that the *Phormidium* cyanobacterial material was unialgal before transferring a subsample to a sterile plastic vial filled with 0.2-μm-filtered lake water. This *Phormidium* culture was stored at ambient indoor light at the lakeside laboratory for approximately 10 days and then shipped to the Natural History Museum, where it was cultured in BG11 liquid medium under ambient room light at approximately 15°C. DNA was extracted using the MoBio Powerbio DNA extraction kit according to the manufacturer's instructions. A portion of the 16S rRNA gene was amplified using the protocol described by Taton et al. (21), and the product was sequenced using the primers 809R (51) and 1494R (21) at the Natural History Museum sequencing facility using an Applied Biosystems 3730xl DNA Analyzer (Applied Biosystems, Foster City, CA).

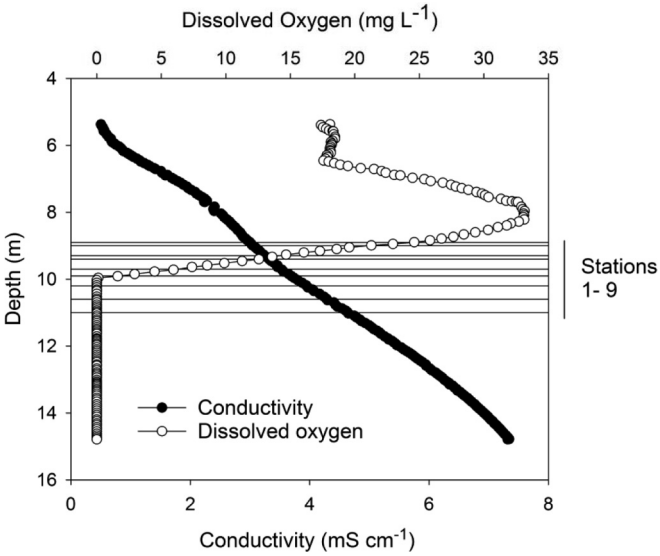

FIG 2 Profile of conductivity (mS cm^{-1}) and dissolved oxygen (mg $liter^{-1}$) by depth in Lake Fryxell. Superimposed are the depths of the nine transect stations.

For the phylogenetic analysis, the partial 16S rRNA gene sequence (~1,000 bp) was aligned with reference sequences using Clustal X (version 2.0.9). For comparison, *Oscillatoria*, *Phormidium*, *Tychonema*, and *Microcoleus* references strains isolated from Antarctic and temperate environments were selected. Manual editing was carried out with MacClade 4.08 (53). Phylogenetic trees were constructed using maximum likelihood (ML) with RAXML-HPC2 on TG (7.2.8; CIPRES Science Gateway V 3.0.x) (54), and the GTRCAT substitution model was used for the bootstrapping phase. A best-scoring ML tree was obtained with 1,000 bootstraps. The 11-bp insertion (5′-AGTTGTGAAAG-3′) (55) was removed from the alignment.

Nucleotide sequence accession numbers. The high-throughput sequencing data were submitted to the Sequence Read Archive (SRA) in GenBank under BioProject PRJNA291280. The 16S rRNA gene sequence has GenBank accession number KT347094.

RESULTS

Water properties and PAR. Conductivity profiles confirmed that the lake was stably stratified along the transect, which ran from 8.9 to 11.0 m in depth. Conductivity increased with depth from stations 1 to 9 along the transect, from 3 to 4.5 mS cm^{-1} (Fig. 2) while temperature varied only between 2.7 and 2.4°C (Table 1). Within this stable profile, the dissolved oxygen concentration fell rapidly from above atmospheric saturation (which is ~14.3 mg $liter^{-1}$ at ambient conditions of 2°C and 3 mS cm^{-1} conductivity as sodium chloride) to zero at ~9.8 m (Table 1; Fig. 2). The upper four transect stations are thus in the oxic part of the lake, stations 5 and 6 are at the oxic-anoxic transition (termed here the oxygen limit), and the final three stations are in anoxic water. Oxygen concentration, dissolved oxygen, and temperature at 50 mm above bottom along the transect were no different from values recorded at similar depths at the center-lake profile. Divers reported smelling sulfide from station 7 downwards.

Along the transect, the pH decreased from 7.50 at 8.9 m (station 1) to a minimum of 7.44 at 9.4 m (station 4), rising with

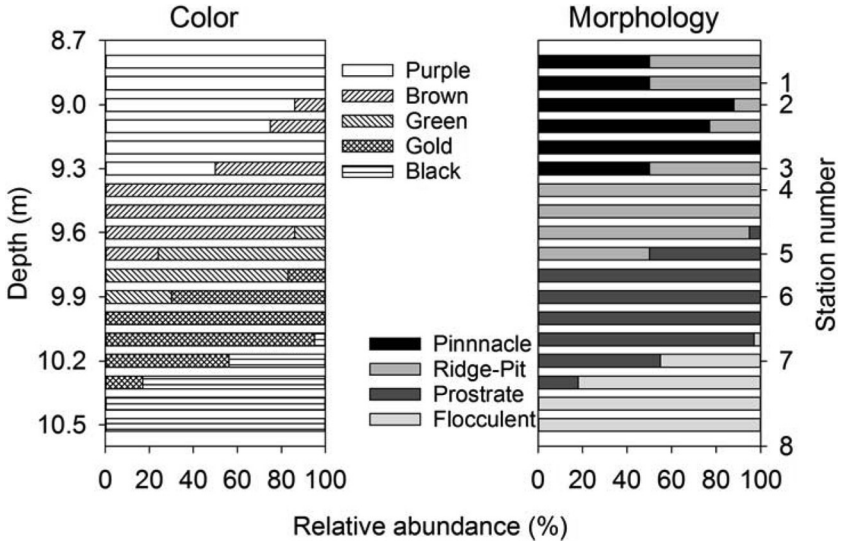

FIG 3 Distributions of common mat colors (left) and types (right) along the transect. At the extreme right are shown the depths of the upper eight transect stations.

increasing depth thereafter to 7.52 at 11.0 m (station 9) (Table 1). DIC increased steadily from 180 to 310 mg liter^{-1}, while dissolved N and P species showed an abrupt increase going from station 6 to 7, coincident with the anoxic interface (Table 1). DRP and NH_4^+ N increased rapidly into the anoxic zone, from low concentrations in the oxic waters, while NO_3^- N remained at low concentrations throughout the transect.

Irradiance transmission through the ice averaged 2.8% ± 1.0% (mean ± standard deviation) (range, 1.3 to 4.2%; $n = 25$). Attenuation within the water column resulted in a near-exponential decline in irradiance with depth, and a vertical extinction coefficient for downwelling irradiance was calculated as 0.48 m^{-1} (Table 1).

Classification and quantification of macroscopic mat morphology. The benthic microbial community morphology varied with depth, water chemistry, and PAR. Communities were classified into four distinct macroscopic morphologies: pinnacle mat, ridge-pit mat, prostrate mat, and flocculent biomass (see Fig. S1 in the supplemental material):

Pinnacle mats were a pink-purple color and had high relief, with ≤5-cm-tall cuspate pinnacles on centimeter-scale spacings (see Fig. S1A in the supplemental material). These mats were internally laminated, with surface laminae 2 to 3 mm thick, and had at least 5 laminae distinguishable in three differently pigmented zones; colors consisted of an upper pink-purple zone followed by a pale purple middle zone and a beige lower zone (see Fig. S2A in the supplemental material). Laminations were continuous across pinnacle peaks and depressions in the mats. Field microscopy showed that pinnacle mats comprised an assemblage of narrow trichome cyanobacteria, morphologically belonging to genus *Leptolyngbya*, with some organisms belonging to *Pseudanabaena* and *Phormidium*, fewer belonging to *Oscillatoria*, and a sparse but diverse pennate diatom community. This assemblage was present in all laminations of the mat. Pinnacle mats were present from approximately 8.8 to 9.4 m in depth (Fig. 3).

Ridge-pit mats had a flatter relief than pinnacle mats, comprising a network of orange-brown or green ridges separating centimeter-deep, near-round pits of 0.5 to 1.0 cm in diameter, giving a honeycomb-like appearance (see Fig. S1B in the supplemental material). Ridge-pit mats were internally laminated, with the laminae continuous across the ridge-pit morphology, but laminae were very thin (≪1 mm) at the bases of pits and thicker (1 to 2 mm) on ridges (see Fig. S2B in the supplemental material). The upper 2 to 3 laminae were pigmented brown-purple, with several green-beige laminae at depth, followed by a beige zone. Ridge-pit mats were sometimes partially covered in a green pigmented cyanobacterial film. Surface laminae of the ridge-pit mat contained abundant live pennate diatoms, mostly *Diadesmis contenta*, while cyanobacteria morphotypes were referable mostly to *Leptolyngbya* with some belonging to *Phormidium*. Where the green surface layer was present, it was loosely attached and was a near-monospecific thin layer of a *Phormidium* morphotype (6 μm in diameter) similar to that seen on the green prostrate mat (see below). Ridge-pit mats were present from 8.8 to 9.7 m and were the dominant macroscopic morphology from 9.4 to 9.6 m (Fig. 3).

Prostrate mats were flat and either green or orange-brown to golden in color (see Fig. S1C in the supplemental material). The upper zone (≪1-mm thickness) comprised 1 to 3 laminae, followed by ~8 flat green-beige pigmented laminae of <1-mm thickness, and underlain by poorly pigmented and poorly laminated organic matter that appeared to be a decomposing ridge-pit mat (see Fig. S2C in the supplemental material). The superficial green layer of the green prostrate mat comprised the same 6- to 7-μm-diameter *Phormidium* organisms observed overgrowing some ridge-pit mats. Yellow-brown prostrate mats contained diatoms dominated by the pennate diatom *Diadesmis contenta*, all with chloroplasts mostly filling the cell. Prostrate mats were found from 9.6 to 10.3 m and were the dominant morphology in the anoxic zone from 9.8 to 10.1 m of the transect (Fig. 3).

Flocculent biomass was defined by a noncohesive accumulation of dark gray-brown organic material (see Fig. S1D in the supplemental material). Flocculent biomass was indistinctly lam-

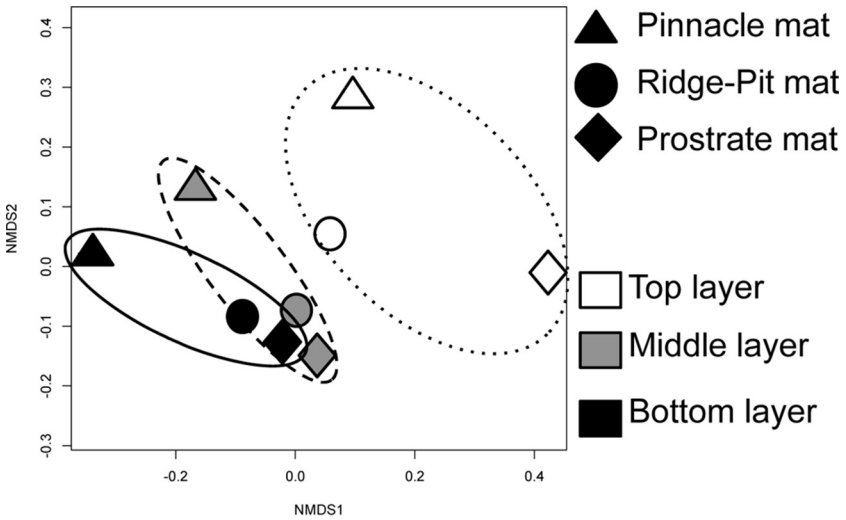

FIG 4 Multidimensional scaling plot derived from standardized OTU abundance in nine benthic samples from Lake Fryxell. Symbol shape indicates the mat type and the position of laminae. Polygons have been added to define the same layer from the three different mat types.

inated with an irregular surface. It was sparsely present at 10.1 m and covered the lake floor from 10.4 m to the end of the transect at 11.0 m (Fig. 3).

The distribution of mat typologies was catalogued from video images, and the results revealed transitions between morphologies occurring at consistent depths on the lake floor (Fig. 3). The depths of the transition from pinnacle or ridge-pit mats to green prostrate, then orange-brown prostrate, and finally flocculent biomass coincided with the shift from oxic to anoxic overlying water. Pinnacle mats and ridge-pit mats were sympatric in part, though the former occurred only at depths where the dissolved oxygen concentration exceeded 7 mg liter^{-1} and the latter only above 0.3 mg liter^{-1}. Green prostate mats occurred only at depths where at most traces of oxygen were present, and golden prostrate mat and flocculent biomass were strictly confined to anoxic water.

Phycoerythrin and chlorophylls. The concentration of the cyanobacterial photosynthetic pigment phycoerythrin decreased from a high at 9.4 m (station 1) and reached near zero at 9.7 m (station 5) (see Fig. S3 in the supplemental material), which coincided with the oxygen limit and the transition from pinnacle and ridge-pit mat to prostrate morphology. In contrast, spectrophotometric estimates of chlorophyll (defined by absorption of acetone extracts at 665 nm) showed a more complex pattern, increasing with depth, including into the anoxic zone. While HPLC showed that Chl *a* was present at all depths, Bchl *c*, *d*, and *e*, which also absorb at 665 nm, were increasingly important with depth. Bchl *c* was greatest at station 5 and below, peaking at station 7, while Bchl e increased steadily from station 7 downwards (see Fig. S3 in the supplemental material). Bchl *d* made a small contribution at all depths. Bchl *a* approximately paralleled Bchl *e*; it first appeared at station 4 (9.4 m) and increased rapidly with depth below the oxygen limit to a maximum at station 9 (11.0 m) (see Fig. S3 in the supplemental material).

Diatom distribution. A diverse (Shannon's index of diversity, >0.5), species-rich diatom flora was present in the benthic microbial mats from 8.9 to 9.3 m (stations 1 to 3), including *Muellaria* spp., *Navicula* spp., *Luticola* spp., *Nitzschia* spp., *Stauroneis* spp., and *Psammothidum* spp. (see Fig. S4 in the supplemental material). Below 9.4 m (station 4), as the oxygen limit was approached and then passed, the diversity rapidly declined, and by 10.2 m (station 7) *Diadesmis contenta* dominated (>97%), with a few individuals of *Navicula gregaria* (Shannon's index of diversity, <0.1). While counts were of cleaned frustules, field microscopy confirmed that living cells of *D. contenta*, with chloroplasts that completely filled cells, were present at 10.2 m and below.

16S rRNA gene microbial mat community composition and distribution. Bacterial and archaeal diversity was characterized using sequencing of 16S rRNA genes. A total of 459,871 sequence reads were used for each sample. Rarefaction curves, Good's coverage, and diversity indices suggested sufficient sampling of the community composition (see Fig. S5 and Table S1 in the supplemental material). Bacterial phyla varied in relative abundance across mat types and mat layers, but no major differences in richness-based diversity indices were observed, and the most abundant phyla were *Bacteroides*, *Proteobacteria*, *Planctomycetes*, *Cyanobacteria*, *Chloroflexi*, *Chlorobi*, and *Verrucomicrobia*. The relative abundance of cyanobacteria declined with layer depth into the mats, particularly in the ridge-pit and prostrate mats (see Fig. S6 in the supplemental material). Nonmetric multidimensional scaling (Fig. 4) based on analysis of 16S rRNA gene OTUs suggests that the upper laminae group separately from the middle and bottom layers. The middle and bottom layers of prostrate and ridge-pit microbial mats were more similar to each other than to the middle and bottom layers of pinnacle mats.

Cyanobacterial 16S rRNA gene diversity across the three mat types (Fig. 5) showed that the mats were dominated by filamentous oscillatorian cyanobacteria with low numbers of potentially nitrogen-fixing OTUs. Of the latter, most were closely related to *Nostoc*. All depths within the pinnacle mat were dominated by *Leptolynbya*, with some *Pseudanabaena*, *Phormidium*, and *Pseudanabaena* organisms present. Relative to the pinnacle mat, the ridge-pit mat samples showed an increase in relative abundance of *Phormidium* (35 to 75%) and reduction in *Leptolynbya* (<45%), with some *Oscillatoria* (5 to 10%), whereas the prostrate mat layers were dominated by *Phormidium* (>80%) and some *Oscillato-*

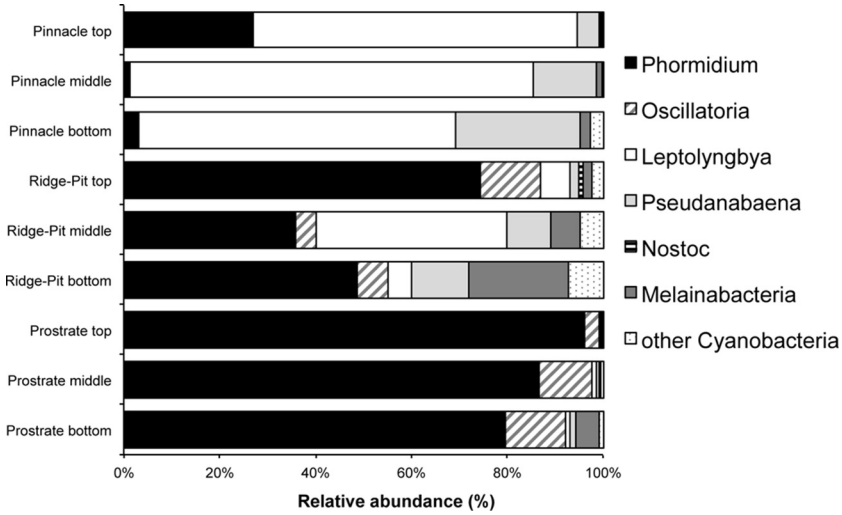

FIG 5 Relative abundances (percent) of major cyanobacterial genera and melainabacteria in the upper, middle, and lower mat layers in pinnacle, ridge-pit, and prostrate mats.

ria organisms (≤15%), and *Leptolynbya* had a relative abundance of ≤3% in all prostrate mat layers.

The thin green biofilm sampled from the top of prostrate mats at 10.4 m was comprised almost entirely of cyanobacterial 16S rRNA genes related to *Phormidium*. 16S rRNA gene phylogenetic analysis of the *Phormidium* isolated from this sample showed that it was related to the previously isolated cyanobacterial strains *Oscillatoria* Ant-Salt, *Oscillatoria* Ant-G17, and *Phormidium* Brack-2 from McMurdo Ice Shelf meltwater ponds near Bratina Island, Antarctica (46), *Oscillatoria acuminata*, and *Phormidium pseudopriestleyi* (previously known as *Oscillatoria priestley*) (see Fig. S7 in the supplemental material).

The relative abundances of the phyla *Proteobacteria* and *Bacteroides* did not show any major changes across mat types and mat layers (see Fig. S8 in the supplemental material). Within the *Proteobacteria*, the mostly heterotrophic *Alpha-*, *Gamma-*, and *Deltaproteobacteria* were most abundant, followed by *Betaproteobacteria*. The relative abundances of these *Proteobacteria* classes were similar across mat type and mat layer. The undescribed TA18 class was also detected and had a relative abundance of 5 to 10% in the pinnacle mat but was <1% or absent in in the ridge-pit and prostrate mats. In contrast, sulfur-oxidizing *Epsilonproteobacteria* appeared only in the prostrate mat that was overlain by anoxic water and in the lowest mat layer in the ridge-pit mat. Even though *Epsilonproteobacteria* were restricted to anoxic subenvironments, other bacterial classes likely to be involved in sulfur metabolism and to contain Bchls were present in all mat types. *Chloroflexi* (green nonsulfur bacteria) and *Chlorobi* (green sulfur bacteria) increased in relative abundance with depth into the mats as well as from the shallower pinnacle to deeper ridge-pit to prostrate mats in the anoxic lake water, with both groups reaching to up to 15% relative abundance.

Archaea were detected, but at very low relative abundance throughout all mat layers. The archaeal composition consisted of OTUs grouping to *Parvarchaea* and *Crenarchaeota* (see Fig. S9 in the supplemental material). All three mat types contained low numbers of 16S rRNA gene sequences related to *Melainabacteria*, a recently identified and still-uncultured phylum (Fig. 5).

DISCUSSION

Distinct microbial mat assemblages along an environmental gradient. Distinctive transitions in the microbial composition and mat morphologies were seen along the depth transect. Mats changed from pink-purple pinnacle mats in the upper, oxic part of the transect to an orange-brown ridge-pit morphology toward the oxygen limit and finally to green and golden prostrate microbial mats in anoxic/euxinic waters along the gently sloping lake floor. Dominant morphospecies of cyanobacteria and diatoms, as well as pigment complements, were associated with these shifts in macroscopic mat morphologies. The pink pinnacle mats at 8.9- to 9.3-m depth (stations 1 to 3) were characterized by an abundance of phycoerythrin-rich *Leptolyngbya* morphotypes and a diverse diatom flora. By 9.4 m (station 4), the ridge-pit mat, dominated by *Leptolyngbya*, was replaced by phycoerythrin-poor, green *Phormidium* morphotypes, and a single diatom, *Diadesmis contenta*, was abundant. At the end of the transect, in prostrate mats from the euxinic zone, cyanobacteria were uncommon and bacteriochlorophylls, including Bchl *a*, *c*, *d*, and *e*, all of which can be present in sulfur bacteria (56), were increasingly abundant. Bacterial chlorophyll *e* has previously been shown to be the primary light-transducing pigment in sulfide-oxidizing bacteria growing at extremely low irradiance in the Black Sea (57). Many cyanobacteria and diatoms are motile and able to migrate to more favorable environmental conditions. Therefore, the presence of the single diatom *D. contenta* in the euxinic zone, but more diverse diatoms in oxygenated mats, suggests that the ability to tolerate prolonged exposure to sulfide is restricted to *D. contenta*. Although sulfide tolerance is not a universal property of diatoms, it has been documented in diatoms from other environments in previous studies (see, e.g., references 58 and 59).

Molecular analysis of representative mat types confirmed the shift in cyanobacterial dominance and a reduction in diversity from *Leptolyngbya* in pinnacle mats toward *Phormidium* in ridge-pit and prostrate mats. The suite of cyanobacteria in the pinnacle mats includes a diversity of genera, including *Leptolyngbya*, *Phormidium*, and *Pseudanabaena*. These genera are all common in oxic

MDV lake mats under perennial ice cover, where similar pink microbial mats with pinnacles are common (13, 22). These ribotypes have all also previously been found in the shallow moat mat from Lake Fryxell (21). Shallow moat mats also contain abundant nitrogen-fixing *Nostocales* (21), but under the ice cover, few OTUs were present. Given the very low dissolved inorganic nitrogen in Lake Fryxell above the oxygen limit, the near absence of nitrogen-fixing cyanobacteria is at first surprising. Nitrogen fixers are, however, rare under lake ice in general (18, 23), perhaps because nitrogen fixation is an energetically costly process and low irradiance under permanent ice may preclude any nutritional advantage (22). Our findings thus support the view that the under-ice cyanobacterial flora of the oxic parts of the MDV lakes is largely dominated by genera of *Oscillatoriales* and particularly phycoerythrin-rich *Leptolyngbya*.

Interestingly, the *Phormidium* species dominant in low-oxygen to anoxic ridge-pit and prostrate mats was identified as *P. pseudopriestleyi*. This taxon has been previously been found in high abundance only in shallow hypersaline meltwater ponds on the McMurdo Ice Shelf, Antarctica (60). Those ponds have elevated sulfide levels, due to the presence of organic sediments rich in sodium sulfate salts, suggesting that *P. pseudopriestleyi* has a high tolerance for sulfide, which is present in some but not all cyanobacteria (61, 72). It has been suggested that *Phormidium* spp. may have the ability to photosynthesize both oxygenically and anoxygenically by switching to H_2S as an electron donor in anoxic sumps in Lake Huron, Canada (62). Lake Fryxell is the first reported MDV lake that supports microbial mats with a high abundance of *P. pseudopriestleyi*, and metabolic flexibility to use H_2S as a donor would be advantageous in Lake Fryxell since it would allow photosynthetic growth during periods when there was insufficient light for oxygenic photosynthesis. The dominance of *P. pseudopriestleyi* where the oxygen limit intersects the base of the photic zone is consistent with this interpretation.

Our work presents the first molecular assessment of microbial mat composition in the anoxic part of an MDV lake. There is a clear zonation of benthic mats with depth, and MDS separates the top layers of mats in contact with lake water from the middle and lower mat layers. The relatively lower abundance of cyanobacteria in the top layer of the pinnacle and ridge-pit mats relative to the macroscopic abundance may be due to PCR bias or to a potentially higher contribution of genetic material by heterotrophic bacteria, especially *Proteobacteria*, to the system, as suggested by Varin et al. (63). The increasing abundance of anoxygenic photosynthesizers, such as *Chlorobi*, in the ridge-pit and prostrate mats relative to the shallower pinnacle mat is consistent with the shift in pigments, which implies a change in dominant metabolism from oxygenic to anoxygenic photosynthesis. A similar transition to sulfur metabolism at this depth in Lake Fryxell is seen in planktonic microbial communities (6). The abundance of *Chloroflexi* in the presence of oxygen in the top layer of the pinnacle mat cannot be readily explained but might be linked to spatial variability of oxygen concentrations not captured by the oxygen measurements or due to biomass accumulating during more anoxic conditions during the winter months. While no measurements of sulfide were made in our study, there were regular reports of sulfide being smelled by divers at and in samples returned from 9.9 to 10.3 m (stations 6 to 7), which suggests that waters below the oxygen minimum were euxinic. This is consistent with other studies where sulfide has been measured immediately below the oxygen minimum in Lake Fryxell (6).

Our understanding of freshwater and marine microbial mat function and organization is based more on shallow and intertidal communities from full-sun habitats than on those from the dimly illuminated ones that we describe here. In brightly lit habitats, vertical zonation of organisms and functions within mats in response to light gradients is well understood (38). Many microbial mats and microbialites show strong stratifications of distinct microbial assemblages across mat layers, and mat diversity often shifts along light and temperature gradients (64–66), which was observed to some extent in Lake Fryxell mats. However, in the low-light environments of the ridge-pit and prostrate mats, we also observed a convergence in community composition within middle and bottom laminae. Such convergence below the surface layers has been reported by Armitage et al. (67), where it was interpreted as habitat convergence away from the illuminated or episodically oxic part of the mat in salt mashes.

Sumner et al. (28) showed that oxygen penetrates at least 17 mm into the pinnacle mats during the austral summer. In addition, prostrate mats from below the water column oxygen limit contain some oxygen in the upper millimeters, which is likely produced locally by the *P. pseudopriestleyi*-dominated cyanobacterial community. The presence of oxygen in the deeper layers of the pinnacle mats may in part explain the failure of lower laminae to be dominated by anaerobes. The presence of oxygen may also explain the persistence of high species richness in lower laminae of these mats, in contrast to a microbialite-forming mat from a hypersaline lake on the Kiritimati Atoll, Central Pacific, where bacterial diversity decreased with increasing depth in the mat (65).

Relationship between macroscopic mat morphologies and microbial mat composition. We documented here that the shift in microbial mat composition was accompanied by a significant change in mat morphology from pinnacle mats in shallow hyperoxic water to flat prostrate mats in poorly illuminated, anoxic waters, a transition that has been observed in few other aquatic habitats to date. This shift in morphology is likely due to the stable water chemistry and physical conditions along the gently sloping floor in Lake Fryxell. The mechanism underlying the difference between the low topographic growth of the ridge-pit mat and the high topographic growth form of the pinnacles may relate to the shift in dominance from *Leptolyngbya* to diatoms and *Phormidium*. In the pinnacle mats, vertical extension into pinnacles appears to be characteristic of mats with a higher abundance of *Leptolyngbya*, as documented in previous studies (17, 68), whereas high abundance of *Phormidium* has been more commonly associated with flat prostrate microbial mats in Antarctic lakes (17, 68).

The development of the ridge-pit mat morphology appears to be due to differential growth, with faster vertical growth of the ridges crests than the pit bases. This is evident in the accumulation of annual laminations (11, 13), with accrual on the order of millimeters on the ridges where *D. contenta* and *Phormidium* were concentrated, whereas both were rare in the pit bases, where annual accrual was $\ll$1 mm. Our observations thus support the view that the macroscopic morphology of microbial mats is affected by differential growth, community composition, and behavioral traits (17).

Microbial mat response to environmental change in Lake Fryxell. Our work has consistently shown that the oxic-anoxic boundary of the Lake Fryxell water column is closely associated with lake depth-specific zonation of mat composition. Long-term

persistence of this zonation requires that the depth of the oxygen minimum in the lake water is more or less static, which appears to be largely the case. Consideration of movements of the oxygen minimum requires accommodation of variations in lake level. Since records began in the 1970s, the water level of Lake Fryxell has fluctuated; the lake level showed punctuated rises between 1970 and 1990 (69) but fell gradually during 1991 to 2000, followed by a year of exceptionally high inflow in 2001 to 2002 resulting in a 0.6-m rise, returning the lake to pre-1990 levels (70). The lake level increased by another 0.6 m between 2008 to 2009 and 2011 to 2012 (McMurdo Dry Valleys Long Term Ecological Research, http://www.mcmlter.org/). Thus, the lake is now at least 2 m deeper than it was in 1980, with ~1 m of this rise occurring between 2001 and 2012.

In 1980, the oxygen limit was measured at an approximate depth of 9.5 m, corresponding to a temperature of 3°C, a conductivity of 4 mS cm^{-1}, and an irradiance of ~1 to 2 μmol photons m^{-2} s^{-1} (3). Allowing for 2 m of lake level rise, this is equivalent to a depth of about 11.5 m as measured in 2012. In our data, the oxygen limit was at 9.8-m depth, 2°C, and conductivity of 3.3 mS cm^{-1}, and irradiance was ~1 to 2 μmol photons m^{-2} s^{-1} at the time of sampling. While absolute changes are difficult to reconcile due to changes in instrumentation and techniques between 1980 and 2010, it appears that the oxygen limit has risen relative to the lake floor by 1.7 m, a difference sufficiently large to imply a slow dynamic rise in the oxygen limit. The limit now lies at a similar irradiance but lower conductivity than in 1980, consistent with the oxygen limit location being set by irradiance via the balance of microbial oxygen production and chemical and biological oxygen consumption. The significant rise in lake level between 2001 to 2012 was also accompanied by a period of high turbidity and low irradiance (70). We therefore suggest that the apparent overgrowth of ridge-pit mat by prostrate mat as shown in Fig. S2C in the supplemental material is a record of the decrease in local illumination that accompanied that level rise. Laminations in MDV lake mats are annual (12, 13), and 10 prostrate layers had accumulated by 2012 on top of the ridge-pit, consistent with annual accrual in the 10 years since the 2001 to 2002 flood year. Thus, insofar as the microbial mats in Lake Fryxell are structured by dissolved oxygen concentrations, they may contain a fine-scale record of the dynamics of the lake environment.

In summary, this study revealed a depth-related transect of phototrophic microbial mats that were segregated into three distinct mat morphologies, with associated differences in community composition and dominant imputed physiologies, through the oxycline within the perennially ice-covered Lake Fryxell, Antarctica. The simplest explanation of this distribution is that it is driven by the light-determined limit to which oxygenic photosynthesis can maintain an oxidized environment in the lake's vertically stable water column. The benthic microbial community composition transitioned from pinnacle mats formed by narrow-trichome *Leptolyngbya*, rich in phycoerythrin, to ridge-pit mats and subsequently to prostrate mats dominated by diatoms and *Phormidium pseudopriestleyi* and increasingly by anaerobic metabolisms. Sulfide-tolerant cyanobacteria and diatoms were found that were able to create oxygen-rich, probably seasonal, microhabitats within the mats that maintain aerobic assemblages and thus taxonomic richness. These microbial mats are important systems to elucidate not only microbial diversity but also ecological processes. Correlation between variation of water level and rise of oxygen limits and mat morphologies suggests that these microbial ecosystems may be used as indicators of climate-driven hydrological changes and fundamental biogeochemical boundaries in polar perennially ice-covered lakes.

ACKNOWLEDGMENTS

The 16S rRNA sequence analysis was performed under the MiSeq Competition MkIIm by New Zealand Genome Limited and with the assistance of Patrick Biggs (NZGL) for MiSeq sequence processing. We thank Alexander Forrest for the loan of the Brancker CTD. We are grateful to three anonymous reviewers for their comments and suggestions. We thank the Antarctica New Zealand and U.S. Antarctic Program for logistics support and facilities, and we also thank Anthea Fisher (Antarctica New Zealand) for her assistance with the field work.

The work was supported in part by NSF grant 1115245 to P.T.D., NASA Astrobiology grant NN13AI60G to D.Y.S., and a MiSeq Competition MkIIm by New Zealand Genome limited award to I.H. and A.D.J.

FUNDING INFORMATION

NSF provided funding to Peter T. Doran under grant number 1115245. NASA provided funding to Dawn Sumner under grant number NN13AI60G.

The funders had no role in study design, data collection and interpretation, or the decision to submit the work for publication.

REFERENCES

1. **Priscu JC, Wolf CF, Takacs DC, Fritsen CH, Laybourn-Parry J, Roberts EC, Lyons WB.** 1999. Organic carbon transformations in the water column of a perennially ice-covered Antarctic lake. Bioscience **49:**997–1008. http://dx.doi.org/10.2307/1313733.
2. **Spigel RH, Priscu JC.** 1998. Physical limnology of the McMurdo Dry Valley lakes, p 153–189. *In* Priscu JC (ed), Ecosystem dynamics in a polar desert: the McMurdo Dry Valleys, Antarctica. American Geophysical Union, Washington, DC.
3. **Vincent WF, Downes MT, Vincent CT.** 1981. Nitrous oxide cycling in Lake Vanda, Antarctica. Nature **292:**618–620. http://dx.doi.org/10.1038/292618a0.
4. **Bielewicz S, Bell E, Kong WD, Friedberg I, Priscu JC, Morgan-Kiss RM.** 2011. Protist diversity in a permanently ice-covered Antarctic Lake during the polar night transition. ISME J **5:**1559–1564. http://dx.doi.org/10.1038/ismej.2011.23.
5. **Canfield DE, Green WJ.** 1985. The cycling of nutrients in a closed-basin antarctic lake, Lake Vanda. Biogeochemistry **1:**233–256. http://dx.doi.org/10.1007/BF02187201.
6. **Karr EA, Sattley WM, Jung DO, Madigan MT, Achenbach LA.** 2003. Remarkable diversity of phototrophic purple bacteria in a permanently frozen Antarctic lake. Appl Environ Microbiol **69:**4910–4914. http://dx.doi.org/10.1128/AEM.69.8.4910-4914.2003.
7. **Karr EA, Ng JM, Belchik SM, Sattley WM, Madigan MT, Achenback LA.** 2006. Biodiveristy of methanogenic and other Archaea in permanently frozen Lake Fryxell, Antarctica. Appl Environ Microbiol **72:**1663–1666. http://dx.doi.org/10.1128/AEM.72.2.1663-1666.2006.
8. **Purdy KJ, Hawes I, Bryant CL, Fallick AE, Nedwell DB.** 2001. Estimates of sulphate reduction rates in Lake Vanda, Antarctica support the proposed recent history of the lake. Antarct Sci **13:**393–399.
9. **Vick-Majors TJ, Priscu JC, Amaral-Zettler L.** 2014. Modular structure suggests community plasticity during the transition to polar night in ice-covered Antarctic lakes. ISME J **8:**778–789. http://dx.doi.org/10.1038/ismej.2013.190.
10. **Roberts EC, Laybourn-Parry J, McKnight DM, Novarina G.** 2000. Stratification and dynamics of microbial loop communities in Lake Fryxell, Antarctica. Freshw Biol **44:**649–661. http://dx.doi.org/10.1046/j.1365-2427.2000.00612.x.
11. **Hawes I, Moorhead D, Sutherland D, Schmeling J, Schwarz A-M.** 2001. Benthic primary production in two perennially ice-covered Antarctic lakes: patterns of biomass accumulation with a model of community metabolism. Antarct Sci **13:**18–27.
12. **Hawes I, Schwarz A-M.** 1999. Photosynthesis in an extreme shade environment: benthic microbial mats from Lake Hoare, a permanently ice-

covered Antarctic lake. J Phycol **35:**448–459. http://dx.doi.org/10.1046/j.1529-8817.1999.3530448.x.
13. **Hawes I, Giles H, Doran PT.** 2014. Estimating photosynthetic activity in microbial mats in an ice-covered Antarctic lake using automated oxygen microelectode profiling and variable chlorophyll fluorescence. Limnol Oceanogr **59:**674–688.
14. **Moorhead D, Schmeling J, Hawes I.** 2005. Modeling the contribution of benthic microbial mats to net primary production in Lake Hoare, McMurdo Dry Valleys. Antarct Sci **17:**33–45. http://dx.doi.org/10.1017/S0954102005002403.
15. **Vopel K, Hawes I.** 2006. Photosynthetic performance of benthic microbial mats in Lake Hoare, Antarctica. Limnol Oceanogr **51:**1801–1812. http://dx.doi.org/10.4319/lo.2006.51.4.1801.
16. **Hawes I, Sumner DY, Andersen DT, Jungblut AD, Mackey TJ.** 2013. Timescales of growth response of microbial mats to environmental change in an ice-covered Antarctic lake. Biology **2:**151–176. http://dx.doi.org/10.3390/biology2010151.
17. **Mackey TJ, Sumner DY, Hawes I, Jungblut AD, Andersen DT.** 2015. Growth of modern branched columnar stromatolites in Lake Joyce, Antarctica. Geobiology **13:**373–390. http://dx.doi.org/10.1111/gbi.12138.
18. **Wharton RA, Jr, Parker BC, Simmons GM, Jr.** 1983. Distribution, species composition and morphology of algal mats in Antarctic dry valley lakes. Phycology **22:**355–365. http://dx.doi.org/10.2216/i0031-8884-22-4-355.1.
19. **Jungblut AD, Vincent WF, Lovejoy C.** 2012. Eukaryotes in Arctic and Antarctic cyanbacterial mats. FEMS Microbiol Ecol **82:**416–428. http://dx.doi.org/10.1111/j.1574-6941.2012.01418.x.
20. **Quesada A, Fernández-Valiente E, Hawes I, Howard-Williams C.** 2008. Benthic primary production in polar lakes and rivers, p 179–196. *In* Vincent WF, Laybourn-Parry J (ed), Polar lakes and rivers—Arctic and Antarctic aquatic ecosystems. Oxford University Press, Oxford, United Kingdom.
21. **Taton A, Grubisic S, Brambilla E, De Wit R, Wilmotte A.** 2003. Cyanobacterial diversity in natural and artificial microbial mats of Lake Fryxell (McMurdo Dry Valleys, Antarctica): a morphological and molecular approach. Appl Environ Microbiol **69:**5157–5169. http://dx.doi.org/10.1128/AEM.69.9.5157-5169.2003.
22. **Zhang L, Jungblut AD, Hawes I, Andersen DT, Sumner DY, Mackey TJ.** 2015. Cyanobacterial diversity in benthic mats of the McMurdo Dry Valley Lakes, Antarctica. Polar Biol **38:**1097–1110. http://dx.doi.org/10.1007/s00300-015-1669-0.
23. **Hawes I, Schwarz A-M.** 2001. Absorption and utilization of irradiance by cyanobacterial mats in two ice-covered Antarctic lakes with contrasting light climates. J Phycol **37:**5–15. http://dx.doi.org/10.1046/j.1529-8817.1999.014012005.x.
24. **Sutherland DL, Hawes I.** 2009. Annual growth layers as proxies of past growth conditions for benthic microbial mats in a perennially ice-covered Antarctic lake. FEMS Microb Ecol **67:**279–292. http://dx.doi.org/10.1111/j.1574-6941.2008.00621.x.
25. **Dolhi, JM, Teufel AG, Kong W, Morgan-Kiss RM.** 2015. Diversity and spatial distribution of autotrophic communities within and between ice-covered Antarctic lakes (McMurdo Dry Valleys). Limnol Oceanogr **60:**977–991. http://dx.doi.org/10.1002/lno.10071.
26. **Lyons WB, Welch KA, Snyder G, Olesik J, Graham EY, Marion GM, Poreda RJ.** 2005. Halogen geochemistry of the McMurdo dry valleys lakes, Antarctica: clues to the origin of solutes and lake evolution. Geochim Cosmochim Acta **69:**305–323. http://dx.doi.org/10.1016/j.gca.2004.06.040.
27. **Vincent WF.** 1982. Production strategies in Antarctic inland waters: phytoplankton eco-physiology in a permanently ice-covered lake. Ecology **62:**1215–1224.
28. **Sumner DY, Hawes I, Mackey TJ, Jungblut AD, Doran PT.** 2015. Antarctic microbial mats: a modern analog for Archean lacustrine oxygen oases. Geology **43:**G36966.1. http://dx.doi.org/10.1130/G36966.1.
29. **Aiken G, McKnight D, Harnish R, Wershaw R.** 1996. Geochemistry of aquatic humic substances in Lake Fryxell Basin, Antarctica. Biogeochemistry **34:**157–188.
30. **Dugan HA, Obryk MO, Doran PT.** 2013. Lake ice ablation rates from permanently ice covered Antarctic lakes. J Glaciol **59:**491–498. http://dx.doi.org/10.3189/2013JoG12J080.
31. **Lyons WB, Tyler SW, Wharton RA, Jr, McKnight DM, Vaugh BH.** 1998. A late Holocene desiccation of Lake Hoare and Lake Fryxell, McMurdo Dry Valleys, Antarctica. Antarct Sci **10:**247–256.
32. **Konfirst MA, Sjunneskog C, Scherer RP, Doran PT.** 2011. A diatom record of encironmental change in Fryxell Basin, Taylor Valley, Antarctica, late Pleistocene to present. J Palaeolimnol **46:**257–272. http://dx.doi.org/10.1007/s10933-011-9537-6.
33. **Whittaker TE, Hall BL, Hendy CH, Spaulding SA.** 2008. Holocene depositional environments and surface-level changes at Lake Fryxell, Antarctica. Holocene **18:**775–786. http://dx.doi.org/10.1177/0959683608091797.
34. **Priscu JC.** 1995. Phytoplankton nutrient deficiency in lakes of the McMurdo dry valleys, Antarctica. Freshw Biol **34:**215–227. http://dx.doi.org/10.1111/j.1365-2427.1995.tb00882.x.
35. **Howard-Williams C, Schwarz A-M, Hawes I.** 1998. Optical properties of the McMurdo Dry Valley Lakes, Antarctica, p 189–205. *In* Priscu JC (ed), Ecosystem dynamics in a Polar desert: the McMurdo Dry Valleys, Antarctica. American Geophysical Union, Washington, DC.
36. **Lawrence MJF, Hendy CH.** 1985. Water column and sediment characteristics of Lake Fryxell, Taylor Valley, Antarctica. N Z J Geol Geophys **28:**543–552. http://dx.doi.org/10.1080/00288306.1985.10421206.
37. **Kirk JTO.** 1994. Light and photosynthesis in aquatic ecosystems, 2nd ed. Cambridge University Press, Cambridge, United Kingdom.
38. **Revsbech NP.** 1989. An oxygen microelectrode with a guard cathode. Limnol Oceanogr **34:**472–476.
39. **Komarek J, Anagnostidis K.** 1989. Modern approach to the classification system of cyanophytes 4—Nostocales. Arch Hydrobiol Suppl **82:**247–345.
40. **Komarek J, Anagnostidis K.** 2000. Cyanoprokaryota. Teil 1, Chroococcales. Gustav Fisher, Jena, Germany.
41. **Komarek J, Anagnostidis K.** 2005. Cyanoprokaryota. Teil 2, Oscillatoriales. Gustav Fisher, Jena, Germany.
42. **Downes MT, Hall JA.** 1998. A sensitive fluorometric technique for the measurement of phycobilin pigments and its application to the study of marine and freshwater picophytoplankton in oligotrophic environments, J Appl Phycol **10:**357–363.
43. **Marker AF, Crowther CA, Gunn RJM.** 1980. Methanol and acetone as solvents for estimation chlorophyll-a and phaeopigments by spectrophotomery. Ergebn Limnol **14:**52–69.
44. **Scheer H.** 2006. An overview of chlorophylls and bacteriochlorophylls: biochemistry, biophysics, functions and applications, p 1–26. *In* Grimm B, Porra RJ, Rüdiger W, Scheer H (ed), Chlorophylls and bacteriochlorophylls: biochemistry, biophysics, functions and applications. Springer, Dordrecht, The Netherlands.
45. **Hawes I, Sumner DY, Andersen DT, Mackey TJ.** 2011. Legacies of recent environmental change in the benthic communities of Lake Joyce, a perennially ice covered Antarctic lake. Geobiology **9:**394–410. http://dx.doi.org/10.1111/j.1472-4669.2011.00289.x.
46. **Spaulding SA, McKnight DM, Stoermer EF, Doran PT.** 1997. Diatoms in sediment of perennially ice-covered Lake Hoare, and implications for interpreting lake history in the McMurdo Dry Valleys of Antarctica. J Paleolimnol **17:**403–420.
47. **Caporaso JG, Kuczynski J, Stombaugh J, Bittinger K, Bushman FD, Costello EK, Fierer N, Gonzalez Peña A, Goodrich JK, Gordon JI, Huttley GA, Kelley ST, Knights D, Koenig JE, Ley RE, Lozupone CA, McDonald D, Muegge BD, Pirrung M, Reeder J, Sevinsky JR, Turnbaugh PJ, Walters WA, Widmann J, Yatsunenko T, Zaneveld J, Knight R.** 2010. QIIME allows analysis of high-throughput community sequencing data. Nat Methods **7:**335–336. http://dx.doi.org/10.1038/nmeth.f.303.
48. **Cox MP, Peterson DA, Biggs PA.** 2010. SolexaQA: at-a-glance quality assessment of Illumina second-generation sequencing data. BMC Genomics **11:**485. http://dx.doi.org/10.1186/1471-2164-11-485.
49. **Magoc T, Salzberg SL.** 2011. FLASH: fast length adjustment of short reads to improve genome assemblies. Bioinformatics **27:**2957–2963. http://dx.doi.org/10.1093/bioinformatics/btr507.
50. **Caporaso JG, Bittinger K, Bushman FD, DeSantis TZ, Andersen GL, Knight R.** 2010. PyNAST: a flexible tool for aligning sequences to a template alignment. Bioinformatics **26:**266–267. http://dx.doi.org/10.1093/bioinformatics/btp636.
51. **Quast C, Pruesse E, Yilmaz P, Gerken J, Schweer T, Yarza P, Peplies J, Glöckner FO.** 2013. The SILVA ribosomal RNA gene database project: improved data processing and web-based tools. Nucleic Acids Res **41**(D1)**:**D590–D596. http://dx.doi.org/10.1093/nar/gks1219.
52. **Oksanen JF, Blanchet G, Kindt R, Legendre P, Minchin PR, O'Hara RB, Simpson GL, Solymos P, Henry Wagner MHS, Wagner H.** 2015. vegan: Community Ecology Package. R package version 2.2-1. http://CRAN.R-project.org/package=vegan.
53. **Maddison D, Maddison W.** 2002. MacClade: analysis of phylogeny and character evolution (version 4.08). Sinauer Associates, Sunderland, MA.

54. **Stamatakis A, Hoover P, Rougemont J.** 2008. A rapid bootstrap algorithm for the RAxML web servers. Syst Biol **57:**758–771. http://dx.doi.org/10.1080/10635150802429642.
55. **Nadeau TL, Milbrandt EC, Castenholz RW.** 2001. Evolutionary relationships of cultivated Antarctic oscillatorians (cyanobacteria). J Phycol **37:**650–654. http://dx.doi.org/10.1046/j.1529-8817.2001.037004650.x.
56. **Olsen JM.** 1998. Chlorophyll organization and funciton in green photosynthetic bacteria. Photochem Photobiol **67:**61–75. http://dx.doi.org/10.1111/j.1751-1097.1998.tb05166.x.
57. **Overmann J, Cypionka A, Pfennig N.** 1992. An extremely low-light adapted phototropic sulfur bacterium from the Black Sea. Limnol Oceanogr **37:**150–155. http://dx.doi.org/10.4319/lo.1992.37.1.0150.
58. **Admiraal W, Peletier H.** 1979. Sulphide tolerance of benthic diatoms in relation to their distribution in an estuary. Br Phycol J **14:**185–196. http://dx.doi.org/10.1080/00071617900650201.
59. **Ciglenečki IM, Plavšić M, Vojvodić V, Ćosović B, Pepi M, Baldi F.** 2003. Mucopolysaccharide transformation by sulfide in diatom cultures and natural mucilage. Mar Ecol Prog Ser **263:**17–27.
60. **Jungblut AD, Hawes I, Hitzfeld B, Mountfort D, Dietrich D, Burns BP, Neilan BA.** 2005. Diversity within cyanobacterial mat communities in variable salinity meltwater ponds of McMurdo Ice Shelf, Antarctica. Environ Microbiol **7:**519–529. http://dx.doi.org/10.1111/j.1462-2920.2005.00717.x.
61. **Oren A.** 2000. Salt and brines, p 281–306. *In* Whitton BA, Potts M (ed), The ecology of cyanobacteria. Kluwer, Dordrecht, The Netherlands.
62. **Voorhies AA, Biddanda BA, Kendall ST, Jain S, Marcus DN, Nold SC, Sheldon ND, Dick GJ.** 2012. Cyanobacterial life at low O_2: community genomics and function reveal metabolic versatility and extremely low diversity in a Great Lakes sinkhole mat. Geobiology **10:**250–267. http://dx.doi.org/10.1111/j.1472-4669.2012.00322.x.
63. **Varin T, Lovejoy C, Jungblut AD, Vincent WF, Corbeil J.** 2012. Metagenomic analysis of stress genes in microbial mat communities from Antarctica and the high Arctic. Appl Environ Microbiol **78:**549–559. http://dx.doi.org/10.1128/AEM.06354-11.
64. **Couradeau E, Benzerara K, Moreira D, Gérard E, Kaźmierczak J, Tavera R, López-García P.** 2011. Prokaryotic and eukaryotic community structure in field and cultured microbialites from the alkaline lake Alchichica (Mexico). PLoS One **6:**e28767. http://dx.doi.org/10.1371/journal.pone.0028767.
65. **Schneider D, Arp G, Reimer A, Reitner J, Daniel R.** 2013. Phylogenetic analysis of a microbialite-forming microbial mat from a hypersaline lake of the Kiritimati atoll, Central Pacific. PLoS One **8:**e6662. http://dx.doi.org/10.1371/journal.pone.0066662.
66. **Ward DM, Castenholz RW.** 2000. Cyanobacteria in geothermal habitats, p 37–59. *In* Potts M, Whitton B (ed), Ecology of cyanobacteria. Kluwer Academic Publishers, Dordrecht, The Netherlands.
67. **Armitage DW, Gallagher KL, Youngblut ND, Buckley DH, Zinder SH.** 2012. Millimeter-scale patterns of phylogenetic and trait diversity in a salt marsh microbial mat. Front Microbiol **3:**293. http://dx.doi.org/10.3389/fmicb.2012.00293.
68. **Reyes K, Gonzalez NII, Steward J, Ospino F, Nguyen D, Cho D, Ghahremani N, Spear JR, Johnson HA.** 2013. Surface orientation affects the direction of cone growth by Leptolynbya sp. strain C1, a likely architect of coniform structures Octopus Spring (Yellowstone National Park). Appl Environ Microbiol **79:**1302–1308. http://dx.doi.org/10.1128/AEM.03008-12.
69. **Chinn TJ.** 1993. Physical hydrology of the Dry Valley lakes. Antarct Res Ser **59:**1–52. http://dx.doi.org/10.1029/AR059p0001.
70. **Foreman CM, Wolf CF, Priscu JC.** 2004. Impact of episodic warming events on the physical, chemical and biological relationships of lakes in the McMurdo Dry Valleys. Antarct Aquat Geochem **10:**239–268. http://dx.doi.org/10.1007/s10498-004-2261-3.
71. Reference deleted.
72. **Cohen Y, Jorgensen BB, Revsbech NP, Poplawski R.** 1986. Adaptation to hydrogen sulfide of oxygenic and anoxygenic photosynthesis among cyanobacteria. Appl Environ Microbiol **51:**398–407.